Kinetic Study of the Electroreduction of Benzoic Acid

Po-Chung Cheng and Tsutomu Nonaka*

Department of Electronic Chemistry, Graduate School at Nagatsuta, Tokyo Institute of Technology, 4259 Nagatsuta, Midori-ku, Yokohama 226

(Received June 18, 1993)

This work demonstrates the procedures needed to extract kinetic parameters from experimental data and to establish a reasonable model for the electroreduction of benzoic acid in a citrate buffer solution, a reaction typical of consecutive electrochemical reactions with solvent decomposition. Influences of operating conditions (current density, flow rate, etc.) on the formation ratio of benzaldehyde to benzyl alcohol were examined in a flow cell system with a lead cathode. Three reaction mechanism models taking into account dehydration and mass transfer of a hydrated benzaldehyde intermediate were discussed. Numerical calculations showed that the electrolyte in the vicinity of the cathode during an electrolysis was weakly alkaline. Factors controlling the product-selectivity of benzaldehyde are also discussed on the basis of simulation.

The electrolytic reduction of aromatic acids has been a promising process for the preparation of aromatic alcohols and aldehydes.[1—11] In general, the current efficiency is unsatisfactory due to hydrogen evolution and side reactions such as dimerization or oligomerization of the corresponding aldehyde intermediates.[12,13] Furthermore, electrolytic results are significantly influenced by pH, electrode material and supporting electrolyte.[4,6,14] In the electroreduction of benzoic acid at low pH, benzaldehyde is hardly formed.[6,8] However, benzaldehyde can be obtained as a major product in weakly acidic media such as borate or phosphate buffer solutions.[4,5]

The generally-accepted reaction mechanism for the electroreduction of benzoic acid is as follows:[4]

$$\underset{\mathbf{A}}{C_6H_5COOH} \rightleftharpoons \underset{\mathbf{Y}}{C_6H_5COO^-} + H^+ \qquad \text{(I)}$$

$$\underset{\mathbf{A}}{C_6H_5COOH} + 2e + 2H^+ \longrightarrow \underset{\mathbf{B}}{C_6H_5CH(OH)_2} \qquad \text{(II)}$$

$$\underset{\mathbf{B}}{C_6H_5CH(OH)_2} \rightleftharpoons \underset{\mathbf{C}}{C_6H_5CHO} + H_2O \qquad \text{(III)}$$

$$\underset{\mathbf{C}}{C_6H_5CHO} + 2e + 2H^+ \longrightarrow \underset{\mathbf{D}}{C_6H_5CH_2OH} \qquad \text{(IV)}$$

The initial species formed in the reduction of benzoic acid (**A**) is a hydrated benzaldehyde (**B**) which is unreducible.[4,14] Whereas, a dehydrated free benzaldehyde molecule (**C**) is much more reducible than **A**. **B** diffuses from the cathode surface into bulk solution and is dehydrated simultaneously to give **C**; **C** is then converted on the cathode surface into benzyl alcohol **D** as the final product.

It is interesting to investigate control factors for the product-selectivity of benzaldehyde to benzyl alcohol in the electroreduction of benzoic acid and to extend the reduction mechanism to other aromatic acids, because aromatic aldehydes are important intermediates as well as alcohols in organic synthesis. On the other hand, mathematical modeling has not yet been reported for this electrolytic process in spite of the numerous experimental studies. A main reason seems to be that the kinetic analysis of this process involves too many rate expressions and requires delicate control of experimental conditions.

The mass transfer coefficient has been shown to be an important parameter controlling the product-selectivity in electroorganic reactions.[15,16] In the present work, a flow cell with parallel plate electrodes was used since mass transfer can be strictly controlled. Furthermore, numerical simulations based on the above reaction mechanism were performed to clarify the chemical kinetics for the dehydration of hydrated benzaldehyde to benzaldehyde.

Generally, the electroreduction of benzoic acid belongs to a class of consecutive electrochemical reactions with solvent decomposition. This paper aims to establish a methodology for studying the kinetics and predicting the product-selectivity for this type of electroorganic process.

Experimental

Voltammograms were recorded using a DPGS-1 potentiostat (Nikko Keisoku), an HB-104 function generator (Hokuto Denko) and an F-3DH X–Y recorder (Riken Denshi). Measurements were carried out in a divided H-type cell fitted with a lead disk cathode (1 mm in diameter), a platinum plate as the counter electrode and a saturated calomel electrode (SCE) as the reference electrode.

A buffer solution (80 cm^3), composed of 0.2 M (1 M=1

mol dm^{-3}) sodium citrate and 0.05 M H_2SO_4, was used to prepare the catholyte containing 0.1 M benzoic acid. The same buffer solution was used as the anolyte. Preparative electrolyses were performed with a Microflow Cell (ElectroCell AB, Sweden) at 30±2°C. A plastic grid (1/4 inch-mesh) oriented with the axis at 45° to the overall direction of flow was held between a cationic membrane (Ionac MC-3470, Sybron Chemicals Inc., USA) and a lead plate cathode (3.2×3.2 cm) in order to improve turbulence. The electrolytes were circulated with tubing pumps (Masterflex RA-71, Cole-Pamer, USA). Before an electrolysis the flow rate of electrolyte was calibrated.

The products were routinely analyzed using HPLC. The mobile phase was a mixture of acetonitrile and 0.1% aqueous phosphoric acid with a volume ratio of 20:80. The column was a reversed-phase Ultron S-C 18 (Chromato Packings Center) and peaks for the products were detected by UV absorbance at 254 nm. Acrylamide was used as an internal standard.

Results and Discussion

Voltammogram at a Lead Cathode. It is well known that the reduction potential of benzoic acid is rather negative, hence high hydrogen-overvoltage cathodes such as mercury or an amalgam are generally used for producing benzaldehyde in weakly acidic media to avoid hydrogen evolution. Nevertheless, the use of either mercury or an amalgam as the cathode is not preferred from the viewpoint of environmental pollution. Lead is a practical substitute, although its hydrogen overvoltage is lower than Hg. Figure 1, obtained by linear sweep voltammetry (LSV) at a lead cathode, shows that the current efficiency loss due to hydrogen evolution during electroreduction of benzoic acid can be less than 30% in a citrate buffer solution. The current efficiency was found to be satisfactory by preparative electrolysis in an H-type cell. It is most interesting that a considerable amount of benzaldehyde was detected, because this is the first time benzaldehyde was electrolytically produced from benzoic acid at a lead cathode in a weakly acidic solution.

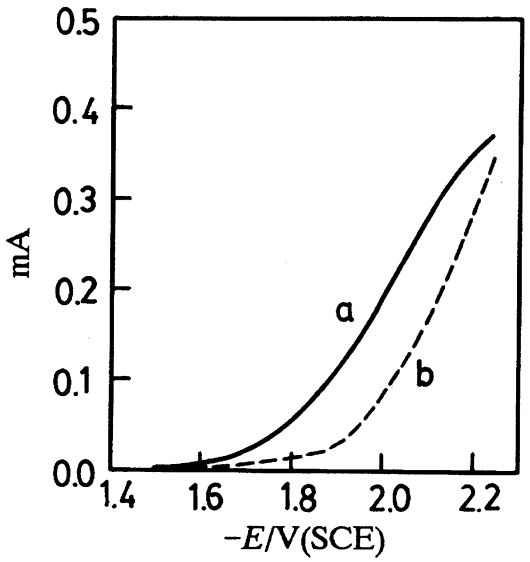

Fig. 1. Voltammograms at 50 mV s^{-1} in citrate buffer solution (0.2 M sodium citrate and 0.05 M H_2SO_4). Curve a, 0.1 M benzoic acid; b, no benzoic acid.

Mass Transfer Processes. The concentration-time behavior in the flow cell system used here can be expressed by Eq. 1 for a simple electrochemical reaction such as the conversion of Ce^{+3} into Ce^{+4} at a current density higher than the mass transfer limiting current density.[17]

$$\ln(c/c_0) = -[1 - \exp(-m\sigma/Q)]Qt/V, \quad (1)$$

where c and t are the substrate concentration and electrolysis time, respectively; c_0 is c at $t=0$; m is the mass transfer coefficient of reactant; Q is the volumetric flow rate of electrolyte; σ is the area of electrode; and V is the total volume of electrolyte in the cell, tubing and reservoir.

Although the electrochemical reaction of benzaldehyde involves both the mass transfer processes of free (**C**) and hydrated benzaldehyde (**B**), the concentration of electrochemically inactive **B** is negligibly small because [**B**] is only 1% of [**C**].[18,19] For this case we can directly use Eq. 1 to obtain the mass transfer coefficient (m_C) of benzaldehyde. The values of m_C in this work was found to obey the Chilton–Colburn analog[20,21] as given by Eq. 2.

$$m_C/\mathrm{cm\,s^{-1}} = 6.8 \times 10^{-5}\ (Q/\mathrm{cm^3\,min^{-1}})^{0.8}. \quad (2)$$

Equation 3 is widely used to describe the concentration–time behavior in a beaker-type batch cell system. If $m\sigma/Q \ll 1$, Eq. 1 can be reduced to Eq. 3. Under our experimental conditions, m_C's calculated from either Eq. 1 or Eq. 3 were found to be essentially the same, and it is therefore reasonable to apply equations derived on the basis of a beaker-type batch cell system to the electrolytic results in this work.

$$\ln(c/c_0) = -m\sigma t/V. \quad (3)$$

On the other hand, the electrochemical reaction of benzoic acid involves the mass transfer processes of benzoic acid (**A**) and benzoate ion (**Y**). However, **A** in a buffer solution (pH≈5) exists mostly as **Y** which is electrochemically inactive, and therefore the mass transfer process of **Y** must be taken into account.

Let $[\mathbf{X}]_b$ and $[\mathbf{X}]_s$ represent the concentrations of species **X** in the bulk solution and on the cathode surface, respectively. The mass transfer rates of **A** and **Y** are defined by

$$N_A = m_A([\mathbf{A}]_b - [\mathbf{A}]_s), \quad (4a)$$

$$N_Y = m_Y([\mathbf{Y}]_b - [\mathbf{Y}]_s), \quad (4b)$$

where N and m are the mass transfer rate and mass transfer coefficient, respectively. Here Eq. 4b is derived

on the assumption that the contribution of migration to the total mass transfer is negligible in comparison with that of convection and diffusion. Although the movement of negatively charged **Y** by migration is toward the anode and hence N_Y is considered less than $m_Y([\mathbf{Y}]_b - [\mathbf{Y}]_s)$, the effect of migration is very small for a system in which mass transfer is dominated by convection.[22] The contribution of migration to the total mass transfer under our experimental conditions is estimated to be less than 3%, even when the concentration of supporting electrolyte is only several times that of **Y**. For this situation the steady-state approximation is applied to **A** and **Y** to give

$$r_1 = k_A[\mathbf{A}]_s = -V\mathrm{d}([\mathbf{A}]_b + [\mathbf{Y}]_b)/\sigma\mathrm{d}t = N_A + N_Y, \quad (5)$$

where r_1 and k_A are the electrochemical reaction rate of benzoic acid and the corresponding reaction rate constant, respectively.

Table 1 shows experimental results at various flow rates and current densities. It is interesting to point out that the formation ratio of benzaldehyde to benzyl alcohol increases with an increase in current density, reaches a maximum at a current density defined as i_{max}, and then drops when $i > i_{max}$. The influence of flow rate is somewhat complicated, however, a higher flow rate evidently produces a higher i_{max}.

From material balance we can write

$$r_1 = -V\mathrm{d}([\mathbf{A}]_b + [\mathbf{Y}]_b)/\sigma\mathrm{d}t = V\mathrm{d}([\mathbf{B}]_b + [\mathbf{C}]_b + [\mathbf{D}]_b)/\sigma\mathrm{d}t. \quad (6)$$

Rearrangement of the data in Table 1 gives Fig. 2 in which r_1 is approximately calculated by

$$r_1 \approx V([C_6H_5CHO]_{0.4} + [C_6H_5CH_2OH]_{0.4})/\sigma t_{0.4}, \quad (7)$$

where $t_{0.4}$ is the electrolysis time when the charge passed is 0.4 F mol^{-1}, and $[C_6H_5CHO]_{0.4}$ and $[C_6H_5CH_2OH]_{0.4}$ are the corresponding concentrations of benzaldehyde and benzyl alcohol, respectively.

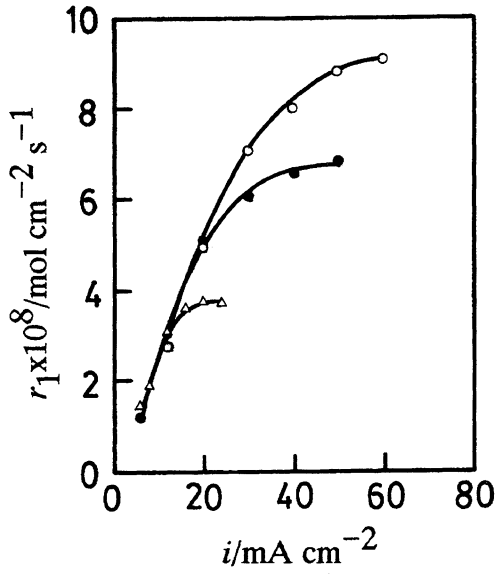

Fig. 2. r_1 vs. i at various flow rates: 100 (△), 200 (●), and 300 (○) cm^3 min^{-1}.

Recognizing that **A** and **Y** are essentially at equilibrium, we have

$$[\mathbf{Y}]_b = K_a[\mathbf{A}]_b/[H^+]_b, \quad (8a)$$

$$[\mathbf{Y}]_s = K_a[\mathbf{A}]_s/[H^+]_s, \quad (8b)$$

where K_a is the acidity of benzoic acid. It is necessary to consider the relationship between $[H^+]_b$ and $[H^+]_s$ in order to obtain further information of the electrochemical reaction of benzoic acid.

Case 1: If the capacity of buffer solution is large enough so that $[H^+]_s = [H^+]_b$, Eq. 9 can be derived from Eqs. 4, 5, and 8 on the reasonable assumption that m_A is equal to m_Y.

$$r_1 = -V\mathrm{d}[\mathbf{Z}]_b/\sigma\mathrm{d}t = m_A k_A[\mathbf{Z}]_b/(m_A\theta + k_A), \quad (9)$$

where $\theta = ([H^+]_b + K_a)/[H^+]_b$, and $[\mathbf{Z}]_b = [\mathbf{A}]_b + [\mathbf{Y}]_b$.

As $k_A \to \infty$, r_1 approaches a maximum defined as r_{lim} which corresponds to the limiting current density for the electroreduction of benzoic acid.

$$r_{lim} = m_A[\mathbf{Z}]_b. \quad (10)$$

Integration of Eq. 9 with $k_A \to \infty$ gives

$$[\mathbf{Z}]_b/[\mathbf{Z}]_0 = ([\mathbf{Z}]_0 - [\mathbf{B}]_b - [\mathbf{C}]_b - [\mathbf{D}]_b)/[\mathbf{Z}]_0 = \exp(-m_A\sigma t/V), \quad (11)$$

where $[\mathbf{Z}]_0$ is $[\mathbf{Z}]_b$ at $t=0$. As shown in Fig. 2, r_1 increases with an increase in current density and finally reaches a limiting value which is r_{lim}. Substituting the data corresponding to r_{lim} into Eq. 11 and solving for m_A, one has

$$m_A/\mathrm{cm\,s^{-1}} = 9.8 \times 10^{-6}\ (Q/\mathrm{cm^3\,min^{-1}})^{0.8}. \quad (12)$$

Comparing Eqs. 2 and 12, it is evidently unreasonable that the average value of m_C/m_A is 6.9, since the similarity in molecular volume between **A** and **C** implies that m_C/m_A must be close to 1.

Case 2: If the capacity of the buffer solution is insufficient, $[H^+]_s$ will be smaller than $[H^+]_b$ because protons at the cathode surface are constantly consumed during the electrochemical reaction of **A**. Recognizing that $[\mathbf{Y}]_s \leq [\mathbf{Y}]_b$, it is easily derived from Eq. 8 that $[\mathbf{A}]_s/[H^+]_s \leq [\mathbf{A}]_b/[H^+]_b$. If the consumption of protons is so fast that $[H^+]_b$ becomes very low, it is very likely that the value of $[\mathbf{A}]_s/[H^+]_s$ approaches its maximum, i.e. $[\mathbf{A}]_s/[H^+]_s \approx [\mathbf{A}]_b/[H^+]_b$. In such a case, $[\mathbf{Y}]_s \approx [\mathbf{Y}]_b$ and $N_Y \approx 0$. Then Eq. 5 is approximated as

$$r_1 = -V\mathrm{d}[\mathbf{Z}]_b/\sigma\mathrm{d}t \approx N_A = m_A k_A[\mathbf{Z}]_b/(m_A + k_A)\theta, \quad (13)$$

And r_1 approaches r_{lim} when $k_A \to \infty$, i.e.

$$r_{lim} = m_A[\mathbf{Z}]_b/\theta. \quad (14)$$

Integration of Eq. 13 with $k_A \to \infty$ gives

Table 1. Effects of Volumetrical Flow Rate (Q) and Current Density (i) on Product-Selectivity in Electroreduction of Benzoic Acid at 0.4 F mol^{-1} of Charge Passed

Run	Q	i	Concentration/mmol dm^{-3}		$[C_6H_5CHO]^{a)}$
	cm^3 min^{-1}	mA cm^{-2}	$C_6H_5CHO^{a)}$	$C_6H_5CH_2OH$	$[C_6H_5CH_2OH]$
1	100	6	2.5	6.8	0.36
2	100	8	3.4	5.9	0.57
3	100	12	3.9	6.1	0.64
4	100	16	2.3	6.5	0.35
5	100	20	1.4	5.9	0.24
6	100	24	0.60	5.4	0.11
7	200	6	1.2	6.8	0.18
8	200	12	3.1	6.8	0.46
9	200	20	3.1	6.7	0.46
10	200	30	2.1	5.8	0.37
11	200	40	1.2	5.2	0.22
12	200	50	0.62	4.7	0.13
13	300	12	2.0	6.9	0.29
14	300	20	3.0	6.7	0.45
15	300	30	3.0	6.1	0.50
16	300	40	2.1	5.6	0.38
17	300	50	1.8	5.0	0.36
18	300	60	1.3	4.6	0.27

a) The measured value is assumed to be the sum of [**B**] and [**C**], however, [**B**] is just 1% of [**C**].[18,19)]

$$[\mathbf{Z}]_b/[\mathbf{Z}]_0 = ([\mathbf{Z}]_0 - [\mathbf{B}]_b - [\mathbf{C}]_b - [\mathbf{D}]_b)/[\mathbf{Z}]_0 = \exp(-m_A\sigma t/\theta V). \quad (15)$$

After substituting the data corresponding to r_{lim} into Eq. 15, one can write

$$(m_A/\theta)/\text{cm s}^{-1} = 9.8\times10^{-6}\ (Q/\text{cm}^3\,\text{min}^{-1})^{0.8}. \quad (16)$$

Since the pK_a of benzoic acid is 4.20 (at 25 °C)[23)] and $[H^+]_b \approx 10^{-5}$ M during an electrolysis, θ and m_C/m_A are estimated to be 7.3 and 0.95, respectively. The value of m_C/m_A is reasonable, hence it is possible that $[\mathbf{A}]_s/[H^+]_s \approx [\mathbf{A}]_b/[H^+]_b = 1400$ and $N_Y \approx 0$ under our experimental conditions.

Electrochemical Kinetics. From the above discussion, the reaction rate of benzoic acid is represented by Eq. 13. The k_A can be determined experimentally by Eq. 17, which is obtained by substituting Eq. 14 into Eq. 13.

$$k_A = m_A/(r_{lim}/r_1 - 1). \quad (17)$$

Let i_H and i be the partial current densities for hydrogen evolution and the total current density, respectively. From material and charge balances, i_H can be obtained from experimental data using Eq. 18.

$$i_H = i - 2FV\text{d}([\mathbf{B}]_b + [\mathbf{C}]_b)/\sigma\text{d}t - 4FV\text{d}[\mathbf{D}]_b/\sigma\text{d}t. \quad (18)$$

Assuming Tafel kinetics we can write

$$k_A = k^0 \exp(-b_1 E), \quad (19)$$

$$i_H = k_H \exp(-b_H E), \quad (20)$$

where k^0, b_1, k_H, and b_H are characteristic constants; E is cathode potential. Then the relation between k_A and i_H is expressed by Eq. 21.

$$\ln i_H = a + \Gamma \ln k_A, \quad (21)$$

where $a = \ln k_H - b_H \ln k^0/b_1$ and $\Gamma = b_H/b_1$.

Absolute values of E, k^0, b_1, k_H, and b_H are not necessary for a model simulation if a and Γ are known. From a plot of $\ln i_H$ vs. $\ln k_A$ (Fig. 3), a and Γ were calculated to be −2.94 and 0.59, respectively.

Dehydration Reaction. The primary product **B** dehydrates when it diffuses from the cathode surface into the bulk solution. For a sufficiently large rate constant for dehydration (k_d), the dehydration can be viewed to occur only in a so-called reaction layer (δ_R), which is thinner than the Nernst diffusion layer (δ_N).

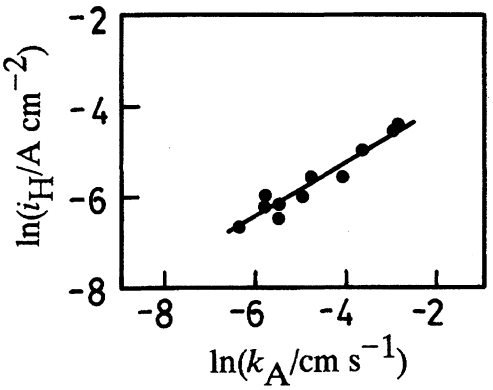

Fig. 3. The relation between i_H and k_A based on the data of Table 1.

Also, for fast dehydration kinetics **B** and **C** in bulk solution are in equilibrium. In such a case, we can write the following equations on the assumption of a steady-state approximation.

$$D_B(d^2[B]/dx^2) - k_d[B] + k_h[C] = 0, \quad (22)$$

$$D_C(d^2[C]/dx^2) - k_h[C] + k_d[B] = 0, \quad (23)$$

$$[B] = [B]_s,\ [C] = 0 \quad \text{at } x = 0, \quad (24a)$$

$$[B] = [B]_b = K_{hyd}[C]_b,\ [C] = [C]_b \quad \text{as } x \to \infty, \quad (24b)$$

where D is the diffusivity, x is the distance from the cathode surface, and k_d and k_h are rate constants for the dehydration of **B** and the hydration of **C**, respectively. The equilibrium constant K_{hyd} is defined as $K_{hyd}=k_h/k_d$. When $D_B=D_C$ and k_d is a constant, Eqs. 25 and 26 are obtained:

$$[B] = f_B(x) = (K_{hyd} + e^{-\alpha x})[C]_b, \quad (25)$$

$$[C] = f_C(x) = (1 - e^{-\alpha x})[C]_b, \quad (26)$$

where $\alpha=\sqrt{(1+K_{hyd})k_d/D_C}$. Then the reaction layer is defined as

$$\delta_R = ([B]_b - [B]_s)/f'_B(0) = 1/\alpha, \quad (27)$$

where $f'_B(x)=df_B/dx$. And

$$\delta_N/\delta_R = (D_C/m_C)\alpha = \sqrt{k_d D_C(1 + K_{hyd})}/m_C. \quad (28)$$

The development of the following reaction models is based on the magnitude of δ_N relative to δ_R. Equation 28 has been derived on the assumption that $\delta_N>\delta_R$. It is evident from Eq. 28 that k_d must not be less than 1 s^{-1} for $\delta_N>\delta_R$ under our experimental conditions.

Model 1: When k_d is so small that **B** dehydrates mainly in the bulk solution, i.e. $\delta_N<\delta_R$ and $k_d<1$ s^{-1} (Eq. 28), the application of the steady-state approximation to species **B** at the cathode surface gives

$$m_A k_A[Z]_b/(m_A + k_A)\theta = m_C([B]_s - [B]_b). \quad (29)$$

Here, the mass transfer coefficient of **B** is reasonably assumed to be the same as m_C. In fact, the k_d's of benzaldehyde derivatives in a solution of pH=5—7 are generally in a range of 0.01 to 0.1 s^{-1}.[18]

The following equations can be obtained from material balances on species **B**, **C**, and **D**.

$$d[B]_b/dt = m_C\sigma([B]_s - [B]_b)/V - k_d[B]_b + k_h[C]_b, \quad (30)$$

$$d[C]_b/dt = -m_C\sigma[C]_b/V + k_d[B]_b - k_h[C]_b, \quad (31)$$

$$d[D]_b/dt = m_C\sigma[C]_b/V. \quad (32)$$

Since **C** is more reducible than **A**, **C** is immediately converted to **D** on the cathode surface and the concentration of **C** at the cathode is considered to be near zero.

The hydration–dehydration equilibrium constant K_{hyd} ($=k_h/k_d$) is reported to be 0.011[19] at 25 °C. If k_d is known, we can simulate the electrolytic results by means of a numerical method as shown in Fig. 4.

However, we found that the predicted values of $([B]_b+[C]_b)/[D]_b$ in this model were much larger than those obtained experimentally. The failure of Model 1 suggests that dehydration occurs mainly in the vicinity of cathode.

Model 2: As described above in the **mass transfer processes** section, $[H^+]_s$ is much lower than $[H^+]_b$. The assumption of $k_d>1$ s^{-1} is reasonable for benzaldehyde derivatives in a weakly basic solution.[18] If dehydration is complete in the reaction layer and $[B]_b=K_{hyd}[C]_b$, then we can write material balances for $[B]_b$, $[C]_b$, and $[D]_b$ as

$$d([B]_b + [C]_b)/dt = (1 + K_{hyd})d[C]_b/dt = m_A k_A\sigma[Z]_b/(m_A + k_A)\theta V - D_C\sigma[C]_b/\delta_R V, \quad (33)$$

$$d[D]_b/dt = D_C\sigma[C]_b/\delta_R V. \quad (34)$$

A value of k_d can be estimated by numerical methods using the data in Table 1. The calculated k_d was found to vary from 10 to 1000 s^{-1} and to depend on experimental conditions, particularly current density. It is suggested that a higher current density produces a lower $[H^+]$ and a larger value of k_d.

At any rate, a concentration profile for protons should exist in the reaction layer. This means that k_d is not constant and varies significantly through the reaction layer. Therefore, it seems appropriate to make a modification in the model where the dehydration is considered to be a combination of heterogeneous and homogeneous reactions.

Model 3: This model is a modification of Model 1

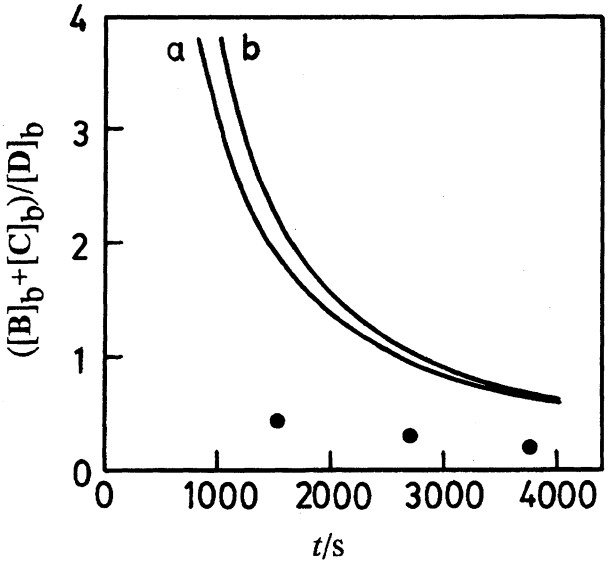

Fig. 4. Calculated (curves) and experimental (plots) time dependencies of product-selectivity under 20 mA cm^{-2} and 200 cm^3 min^{-1}. Simulations were carried out on the basis of Model 1 with k_d=1 and 0.01 s^{-1} for curves a and b, respectively.

described above. In addition to the mass transfer term (i.e. $m_C\sigma[\mathbf{C}]_b/V$), the heterogeneous dehydration of **B** contributes to the formation of **D**. Because **C** is immediately reduced on the cathode surface, $[\mathbf{C}]_s=0$ and the heterogeneous dehydration of **B** yields only benzyl alcohol (**D**). For this situation one can write

$$d[\mathbf{D}]_b/dt = (k_{het}[\mathbf{B}]_s + m_C[\mathbf{C}]_b)\sigma/V, \quad (35)$$

where k_{het} is the rate constant for heterogeneous dehydration.

A steady-state material balance for $\mathbf{B}_s$ leads to

$$m_A k_A[\mathbf{Z}]_b/(m_A+k_A)\theta = m_C([\mathbf{B}]_s - [\mathbf{B}]_b) + k_{het}[\mathbf{B}]_s. \quad (36)$$

It has been shown that k_d is a function of pH.[18] Equation 37a is taken as an approximate expression for k_d in an alkaline solution. Here, the dependence of k_{het} on pH, described as Eq. 37b, is considered to be similar to that for k_d.

$$k_d = c_1 + c_2[OH^-] = c_1 + c_2 \times 10^{-14}/[H^+], \quad (37a)$$

$$k_{het} = \beta_1 + \beta_0/[H^+]_s, \quad (37b)$$

where c_1, c_2, β_1 and β_0 are constants.

From the discussion in the **mass transfer processes** section, it was shown that $[\mathbf{A}]_s/[H^+]_s \approx [\mathbf{A}]_b/[H^+]_b = 1400$, in which case Eq. 37b becomes

$$k_{het} = \beta_1 + \beta_2/[\mathbf{A}]_s, \quad (38)$$

where $\beta_2=1400\beta_0$; $[\mathbf{A}]_s=m_A[\mathbf{Z}]_b/(m_A+k_A)\theta$.

This model's material and charge balance equations for all species are summarized in Table 2. The unknowns k_A and $[\mathbf{B}]_S$ in the rate expressions were calculated from the equation for the steady-state approximation for $[\mathbf{B}]_s$ and from the conservation of charge relationship in Table 2. Since data for k_d of benzaldehyde has not been available, that for 4-chlorobenzaldehyde (ca. 0.03 s^{-1} at 25 °C and pH=5)[18] was used in the numerical simulation. The values of β_1 and β_2 giving the best fit of the theory and experimental data were found to be 2.8×10^{-3} cm s^{-1} and 5.7×10^{-9} mol cm^{-2} s^{-1}, respectively.

Table 2. Summary of Equations and Parameters for Model 3

Rate expressions
$d[\mathbf{Z}]_b/dt=-m_Ak_A\sigma[\mathbf{Z}]_b/(m_A+k_A)\theta V$
$d[\mathbf{B}]_b/dt=m_C\sigma([\mathbf{B}]_s-[\mathbf{B}]_b)/V-k_d[\mathbf{B}]_b+k_h[\mathbf{C}]_b$
$d[\mathbf{C}]_b/dt=-m_C\sigma[\mathbf{C}]_b/V+k_d[\mathbf{B}]_b-k_h[\mathbf{C}]_b$
$d[\mathbf{D}]_b/dt=(k_{het}[\mathbf{B}]_s+m_C[\mathbf{C}]_b)\sigma/V$
Steady-state approximation for $[\mathbf{B}]_s$
$m_Ak_A[\mathbf{Z}]_b/(m_A+k_A)\theta=m_C([\mathbf{B}]_s-[\mathbf{B}]_b)+k_{het}[\mathbf{B}]_s$
Conservation of charges
$i=i_H+2Fm_Ak_A[\mathbf{Z}]_b/(m_A+k_A)\theta+2F(k_{het}[\mathbf{B}]_s+m_C[\mathbf{C}]_b)$
Parameters
$(m_A/\theta)/cm\,s^{-1}=9.8\times10^{-6}\ (Q/cm^3\,min^{-1})^{0.8}$
$m_C/cm\,s^{-1}=6.8\times10^{-5}\ (Q/cm^3\,min^{-1})^{0.8}$
$\theta=([H^+]_b+K_a)/[H^+]_b=7.3$
$i_H/A\,cm^{-2}=e^{-2.94}k_A^{0.59}$
$k_d/s^{-1}=0.030$
$k_h/s^{-1}=k_dK_{hyd}=0.00033$
$k_{het}/cm\,s^{-1}=0.0028+5.7\times10^{-9}\theta(m_A+k_A)/m_A[\mathbf{Z}]_b$

The time dependency of product-selectivity at various flow rates is shown in Fig. 5. The experimental data are generally in good agreement with the calculated results. The ratio of benzaldehyde to benzyl alcohol decreases with an increase in electrolysis time. The effect of flow rate on product-selectivity also has been examined. High flow rates favor the formation of benzaldehyde, if the electrolysis time is not too long. When $t>2500$ s, a higher flow rate (300 vs. 200 $cm^3\,min^{-1}$) leads to lower values of $([\mathbf{B}]_b+[\mathbf{C}]_b)/[\mathbf{D}]_b$ as predicted by the simulation.

The dependence of product-selectivity on current density at various flow rates is also successfully simulated, as shown in Fig. 6. The maximum in product-selectivity is a significant index for testing the validity of the mathematical model. It is important to note that the maximum in product-selectivity is predicted only when Eq. 38 is introduced into the analysis.

Conclusion

The proposed reaction scheme for the electroreduction of benzoic acid has led to a model which is capable of correlating the results observed in flow reactor experiments. It must be emphasized that the electroreduction of benzoic acid belongs to a class of consecutive electrochemical reactions with solvent decomposition. This type of electroorganic process includes a wide range of reactions such as electrooxidation of primary alcohols,

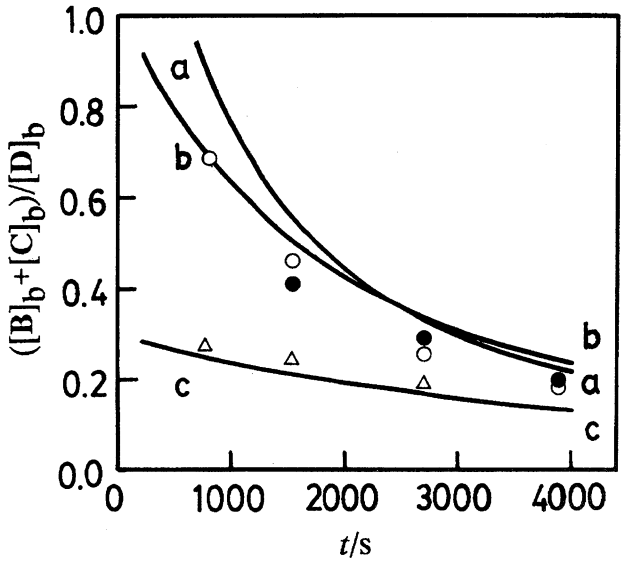

Fig. 5. Calculated (curves) and experimental (plots) time dependencies of product-selectivity under 20 mA cm^{-2}. Simulations were carried out on the basis of Model 3. Flow rate: 300 (a, ○), 200 (b, ●), and 100 (c, △) $cm^3\,min^{-1}$.

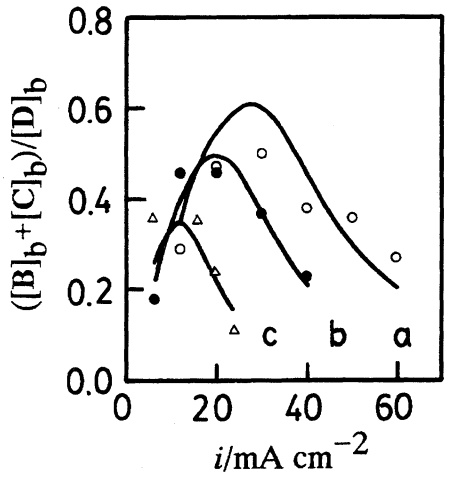

Fig. 6. Calculated (curves) and experimental (plots) current-density dependencies of product-selectivity at 0.4 F mol^{-1}. Flow rate: 300 (a, ○), 200 (b, ●), and 100 (c, △) cm^3 min^{-1}.

electroreduction of benzoic acid derivatives, and electrochemical reactions of polyfunctional compounds. A kinetic approach for this type of electroorganic process has been implemented by the following procedures: (1) studying an individual electrochemical step in differential-conversion experiments to obtain rate information, (2) proposing a possible reaction mechanism model and investigating the chemical reaction of intermediates in an integral-conversion mode, and (3) performing integral-conversion experiments and comparing the results with those predicted by numerical simulation. The complexity of the reaction processes requires some simplifications and modifications, but blind empiricism is not necessary.

The authors wish to thank Professor P. N. Pintauro (Tulane University, USA) for his valuable comments and discussions. The present work was partially supported by a Grant-in-Aid for Scientific Research from the Ministry of Education, Science and Culture, to which the authors are grateful.

References

1) J. A. May and K. J. Kobe, *J. Electrochem. Soc.*, **97**, 183 (1950).
2) H. Lund, *Acta Chem. Scand.*, **17**, 972 (1963).
3) P. Carrahar and F. G. Drakesmith, *J. Chem. Soc., Chem. Commun.*, **1968**, 1562.
4) J. A. Harrison and D. W. Shoesmith, *J. Electroanal. Chem.*, **32**, 125 (1971).
5) J. H. Wagenknecht, *J. Org. Chem.*, **37**, 1513 (1972).
6) R. G. Barradas, O. Kutowy, and D. W. Shoesmith, *Electrochim. Acta*, **19**, 49 (1974).
7) O. R. Brown, J. A. Harrison, and K. S. Sastry, *J. Electroanal. Chem.*, **58**, 387 (1975).
8) I. Taniguchi, A. Yoshiyama, and T. Sekine, *Denki Kagaku*, **45**, 390 (1977).
9) T. Nonaka, T. Kato, T. Fuchigami, and T. Sekine, *Electrochim. Acta*, **26**, 887 (1981).
10) S. Takenaka, Y. Kouno, T. Uchida, and A. Takagi, *Denki Kagaku*, **59**, 570 (1991).
11) N. Sato, A. Yoshiyama, P. -C. Cheng, and T. Nonaka, *J. Appl. Electrochem.*, **22**, 1082 (1992).
12) Z. -H. Wang and Z. -B. Hu, *Electrochim. Acta*, **30**, 779 (1985).
13) M. U. D. Bhatti and O. R. Brown, *J. Electroanal. Chem.*, **68**, 85 (1976).
14) L. Eberson and J. H. P. Utley, "Organic Electrochemistry," 2nd ed, ed by M. M. Baizer and H. Lund, Marcell Dekker, New York (1983), Chap. 11.
15) P. -C. Cheng, T. Nonaka, and T. -C. Chou, *Bull. Chem. Soc. Jpn.*, **64**, 1911 (1991).
16) P. -C. Cheng and T. Nonaka, *Denki Kagaku*, **60**, 131 (1991).
17) R. M. Spotnitz, R. P. Kreh, J. T. Lundquist, and R. J. Press, *J. Appl. Electrochem.*, **20**, 209 (1990).
18) R. A. McClelland and M. Coe, *J. Am. Chem. Soc.*, **105**, 2718 (1983).
19) P. Greenzaid, *J. Org. Chem.*, **38**, 3164 (1973).
20) D. W. Hubbard and E. N. Lightfoot, *Ind. Eng. Chem. Fundam.*, **5**, 370 (1966).
21) D. J. Pickett and K. L. Ong, *Electrochim. Acta*, **19**, 875 (1974).
22) J. S. Newman, "Electrochemical System," 2nd ed, Prentice-Hall, Englewood Cliffs, NJ (1991), Chap. 19.
23) P. D. Bolton, K. A. Fleming, and F. M. Hall, *J. Am. Chem. Soc.*, **94**, 1033 (1972).